VLA Test Memo. No. 213

Calibrating the Site Testing Interferometer

C.L. Carilli, M.A. Holdaway, and A. Roy

National Radio Astronomy Observatory

Socorro, NM, 87801

August 10, 1998

Abstract

Test results indicate that the Site Testing Interferometer data can be used to make a reasonably accurate prediction (within $\approx 30\%$) of the residual rms phase fluctuations at the VLA after Fast Switching phase calibration with a given cycle time, and of the 'turn-off' baseline length for the residual root phase structure function.

1. Introduction

The NRAO site testing interferometer (STIfR) is now operational at the VLA, and software has been installed for real time monitoring of the phase stability (special thanks to T. Folkers, NRAO, Tucson).[1] The STIfR measures continuously the tropospheric contribution to the interferometric phase using an interferometer comprised of two 1.5 m dishes separated by 300 m observing an 11.3 GHz beacon from a geostationary satellite (Radford et al. 1996).

The STIfR measures a time series of phases with an averaging time of 1 s. The real-time analysis software accesses a 600 s time series of phases, removes 360° 'wraps', and fits and removes a quadratic baseline to the time series in order to correct for slow drifts in the satellite position. The software generates a temporal root phase structure function from the data, corresponding to the root mean square (rms) of the phase differences as a function of lag-time for lags from 1 s to 300 s (Holdaway et al. 1995). The software then fits for: (i) a power-law index, α, for short lags, (ii) a constant 'saturation rms', ϕ_{sat}, for long lags, and (iii) the 'corner time', t_{corn}, corresponding to the intersection of the powerlaw and the constant (saturation) functions. The corner time corresponds roughly to the interferometer crossing time for the turbulent phase screen: $t_{corn} \approx \frac{300\ m}{V_A}$, where V_A is the wind speed aloft.

The basic equation for data analysis is the observed power-law dependence of rms phase, ϕ_{rms}, on interferometer baseline length, b:

$$\phi_{rms} = \frac{K}{\lambda}\, b^{\alpha} \qquad (1)$$

where λ is the observing wavelength. The tropospheric-dependent terms are the normalization factor, K, and the power-law index, α. The normalization factor, K, can be

[1]see: http://www.nrao.edu/vla/html/PhaseMonitor

derived from STIfR primary data products by inverting equation 1, and inserting the value of ϕ_{sat}:

$$K = \frac{\lambda_{cm}}{b^{\alpha}} \times \frac{\phi_{sat}}{2^{0.5}} \qquad (2)$$

where $b = 300$ m and $\lambda = 2.7$ cm.[2]

It has been shown that standard phase calibration at the VLA will 'stop' tropospheric phase fluctuations at an effective baseline, $b_{eff} \approx \frac{1}{2} V_A t_{cyc}$ (Carilli and Holdaway 1997), where t_{cyc} is the calibration cycle time. Using the relationship between t_{corn} and V_A given above, this becomes: $b_{eff} = 150$ m $\times \frac{t_{cyc}}{t_{corn}}$. Inserting this expression into (1), and using the measured quantities from the STIfR, we obtain the expected rms phase for the VLA after phase calibration:

$$\phi_{rms} = \frac{1.9}{\lambda_{cm}} \times (\frac{t_{cyc}}{2t_{corn}})^{\alpha} \times \phi_{sat} \qquad (3)$$

This equation can be inverted to give the desired calibration cycle time:

$$t_{cyc} = 2t_{corn} \times (\frac{\lambda_{cm}\phi_{rms}}{1.9\phi_{sat}})^{1/\alpha} \qquad (4)$$

The primary purpose of the STIfR is to serve as a guide to high frequency observers at the VLA. In particular, the STIfR data are meant to be used to estimate the required calibration cycle times when using Fast Switching phase calibration (Holdaway 1992), and

---

[2]The value of ϕ_{sat} is the rms of the lag time series, for which each measurement entails the difference between two interferometer phase measurements at different times. Hence, the rms of the phase lag time series, ϕ_{sat}, is root two larger than the rms of the interferometric phase time series itself, ϕ_{rms}, leading to the extra factor of root two in equation 2. Likewise, since the interferometer phase time series entails the difference in phase between two antennas, the rms of the phase time series, ϕ_{rms}, is another root two larger than rms of the antenna based phase solutions.

in the worst case, to indicate to the observer that high frequency observing may not be possible given the weather conditions.

The purpose of this note is to demonstrate agreement between phase fluctuations measured by the VLA with those measured by the STIfR, and to determine whether predictions based on the temporal root phase structure function as measured by the STIfR agree with the observed spatial root phase structure function observed by the VLA with a given calibration cycle time.

2. Phase Time Series

On June 14, 1997 we observed the celestial calibrator 2229-085 with the C configuration of the VLA while the source passed through conjunction with the satellite. The minimum angular separation between the satellite and the source is 3.1° (satellite declination = -5.6°). The VLA observations were at 15 GHz with a data record length of 1.67 sec. Conjuction of the satellite and the calibrator occured at 12:00 UTC.

The simplest test is to compare the phase time series measured by the STIfR with that measured by the two VLA antennas closest to the STIfR elements. The STIfR is positioned parallel to the east arm of the VLA, and the two closest VLA stations to the STIfR elements are E4 and E8. These antennas are less than 40 m from the STIfR antennas, with a similar baseline length ($\approx$ 300 m), and the same baseline orientation.

The VLA data were self-calibrated on a per-record basis. The phase time series between antennas at E4 and E8 was then reconstructed from the antenna-based phase solutions, and all 4 IFs were included in order to increase the SNR. Using the antenna-based self-calibration phase solutions, and averaging IF's, increases the SNR of the reconstructed interferometric phase time series by a factor of $2 \times (N_{ant} - 2)^{\frac{1}{2}}$ over a single IF time series

of phases on a single baseline.

Figure 1 shows the resulting phase time series between antennas at VLA stations E4 and E8, and the corresponding phase time series from the STIfR, for an hour angle range of ± 30 min around conjunction. The phase fluctuations at 15 GHz have been scaled by the ratio of the frequencies = $\frac{11.3}{15}$. Note the close correlation between the phase variations seen by the two VLA antennas with those seen by the STIfR at times within ± 10 min of conjuction. Also notice how this correlation degrades with increasing hour angle between the source and the satellite. A detailed analysis of these data is in progress to determine the delay that optimizes the cross correlation between these two time series as a function of hour angle. The results can be used to determine the height and velocity of the turbulent layer in the troposphere (Holdaway in prep.).

Figure 2 shows a comparison of the temporal root phase structure functions derived from the VLA and the STIfR data for the 10 minutes of data around conjuction. Again, note the close agreement between the two structure functions. This agreement is not surprising, given the agreement between the phase time series over this time range.

3. Predictions of the STIfR

A second observation was made on July 21, 1998 of the celestial calibrator 2355-106 at 22 GHz in the BnA configuration of the VLA. This source passes within 5° of the satellite, and conjuction with the satellite occured at about 14:00 UTC.

Figure 3 shows the time series of 'standard data products' from the STIfR for July 21, 1998 (0-24 hr UTC), including the saturation rms phase, ϕ_{sat}, the corner time, t_{corn}, and the powerlaw index, α. The mean values for the ± 30 min around conjunction between the satellite and 2355-106 are: $\phi_{sat} = 6° \pm 2°$, $\alpha = 0.6 \pm 0.1$ s, and $t_{corn} = 32 \pm 15$. The corner

time implies a wind velocity of: $v_a \approx \frac{300m}{32s} = 9.4 \pm 4.4$ m/s.

Figure 4 shows the spatial root phase structure function for the VLA data during the time period ± 30 min around conjunction. These are the rms phase values over the full hour integration after application of self-calibration solutions averaged over the full time range (ie. a constant phase term subtracted). This plot shows the three regimes expected for the root struction function (Carilli and Holdaway 1997): (i) the steep rise in RMS phase at short baselines ($\leq$ 1.2 km), corresponding to the 'thick screen' approximation, or 3D turbulence, with b < W, where W = the width of the turbulence, (ii) the more gradual rise at intermediate baselines (1.2 km to 5 km), corresponding to the 'thin screen' approximation, or 2D turbulence, with b > W, and (iii) a flat distribution on the longest baselines ($\geq$ 5 km), corresponding to the outer scale of the turbulence (L_o). Note that we have subtracted (in quadrature) an electronic noise term of 10° (Carilli and Holdaway 1996).

The open cirles in Figure 4 show the root phase structure function after self-calibration with an averaging time of 200 sec. The rms phase values for this self-calibrated data flatten from the nominal root phase structure function at a baseline length of about 1200 ± 200 m, beyond which the rms phases remain constant with baseline length, as expected after calibration. The implied wind velocity is: $v_a \approx \frac{2\times1200m}{200s} = 12 \pm 2$ m/s. The 'saturation' value for the rms phase variations on long baselines is $21^o \pm 3^o$.

The solid line in Figure 4 is the root phase structure function predicted by the mean values for the standard data products from the STIfR. Note that in order to derive this predicted curve we must assume a turbulent layer width (W = 1.2 km), outer scale (L_o = 5 km), and a powerlaw index on intermediate baselines ($\alpha = \frac{1}{3}$). It appears that the assumed powerlaw index on intermediate baselines of $\frac{1}{3}$ is too shallow compared to the VLA data, which leads to an under prediction of the rms phase variations on long baselines. This

discrepancy at long baselines is not a serious problem in practice, since the predicted curve on long baselines is based on a number of assumed variables not measured by the STIfR, and more importantly, only the short baseline part of the curve (the steeply rising portion) is relevant to Fast Switching phase calibration.

The important prediction is the expected 'saturation' value for the rms phase fluctuations after self-calibration. This value is shown as the dash line in Figure 4. The saturation value for the rms phase fluctuations predicted using the STIfR data is $18^\circ \pm 6^\circ$, and the 'turn-off' baseline predicted by the STIfR data is 940 ± 400 m. These values are consistent, within the errors, with the observed values for the spatial root phase structure observed by the VLA, as given above ($21^\circ \pm 3^\circ$, and 1200 ± 200 m, respectively). Overall, these test results indicate that the STIfR data can be used to make a reasonable prediction of the residual rms phase fluctuations at the VLA after Fast Switching phase calibration with a given cycle time, and of the 'turn-off' baseline length for the residual root phase structure function.

The dominant uncertainty in the STIfR data is simply the scatter in the data products over the observed hour, and in particular the scatter in the corner time. The scatter in the corner time may be a result of the fitting algorithm and the 'undulating' behavior of the root structure function at long lag times. We are currently revising the on-line software to allow the user to average the values of the STIfR data products over a specified time range. A second problem is that the data presented herein pertain to sources at the same elevation as the satellite. Holdaway (1998) has considered in detail the statistical behavior of tropospheric phase fluctuations with elevation. We plan to revise the software to correct for source-satellite elevation differences based on his analysis.

References

Carilli, C.L. and Holdaway, M.A. 1997, VLA Scientific Memo. No. 173

Carilli, C.L., Holdaway, M.A., and Sowinski, K. 1996, VLA Scientific Memo. No. 169

Carilli, C.L. and Holdaway, M.A. 1996, VLA Scientific Memo. No. 171

Holdaway, M.A. 1998, MMA Memo. No.221

Holdaway, M.A., Radford, S., Owen, F., and Foster, S. 1995, MMA Memo. 139

Holdaway, M.A. and Owen, F.N. 1995, MMA Memo. No. 126

Holdaway, M.A. Owen, F., and Rupen, M.P. 1994, MMA Memo. No. 123

Holdaway, M.A. 1992, MMA Memo. No. 84

Radford, S.J., Reiland, G., and Shillue, B. 1996, P.A.S.P., 108, 441

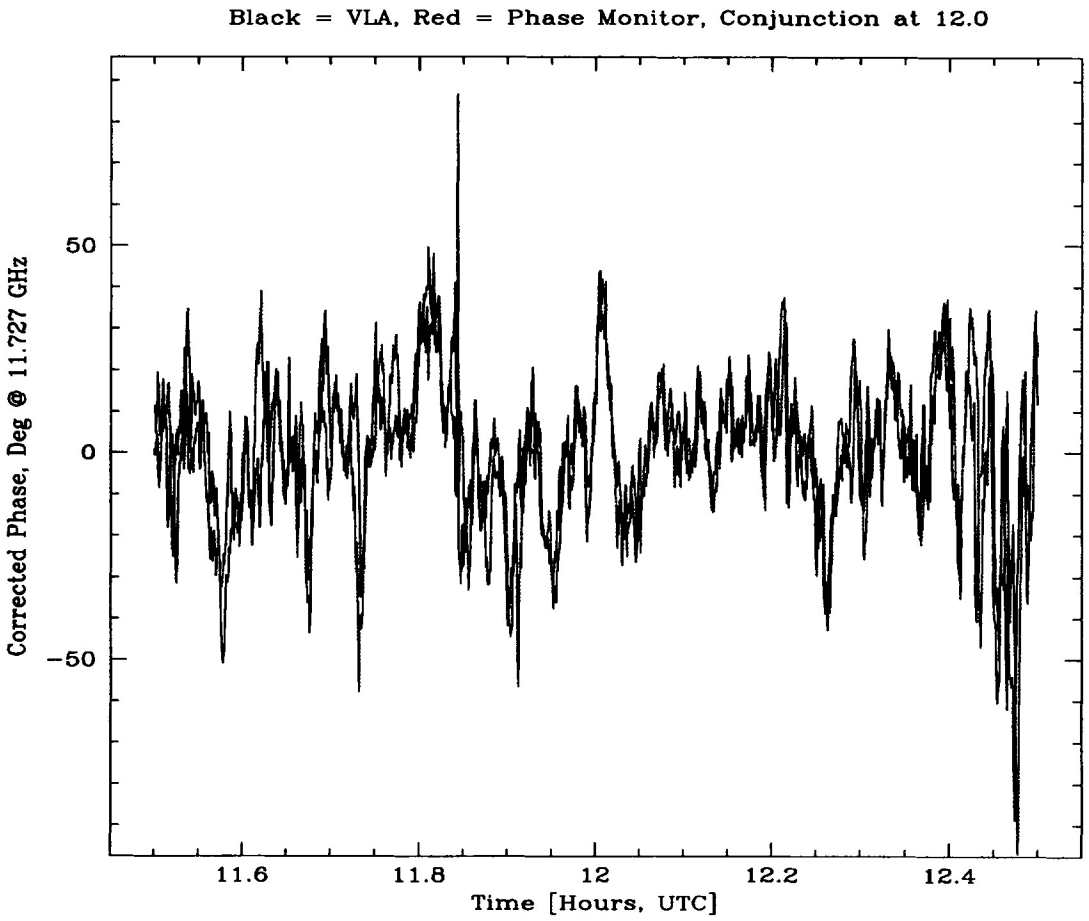

Fig. 1.— The red (dash) line shows the phase time series from the STIfR on June 14, 1997. The black line shows the phase time series for VLA antennas at stations E4 and E8 (adjacent to the STIfR elements) for the same time series as derived at 15 GHz by observating the calibrator 2229-085. Note that the VLA data has been scales by the ratio of the frequencies $= \frac{11.3}{15}$. Conjunction of the satellite and the source occured at 12:00 UTC.

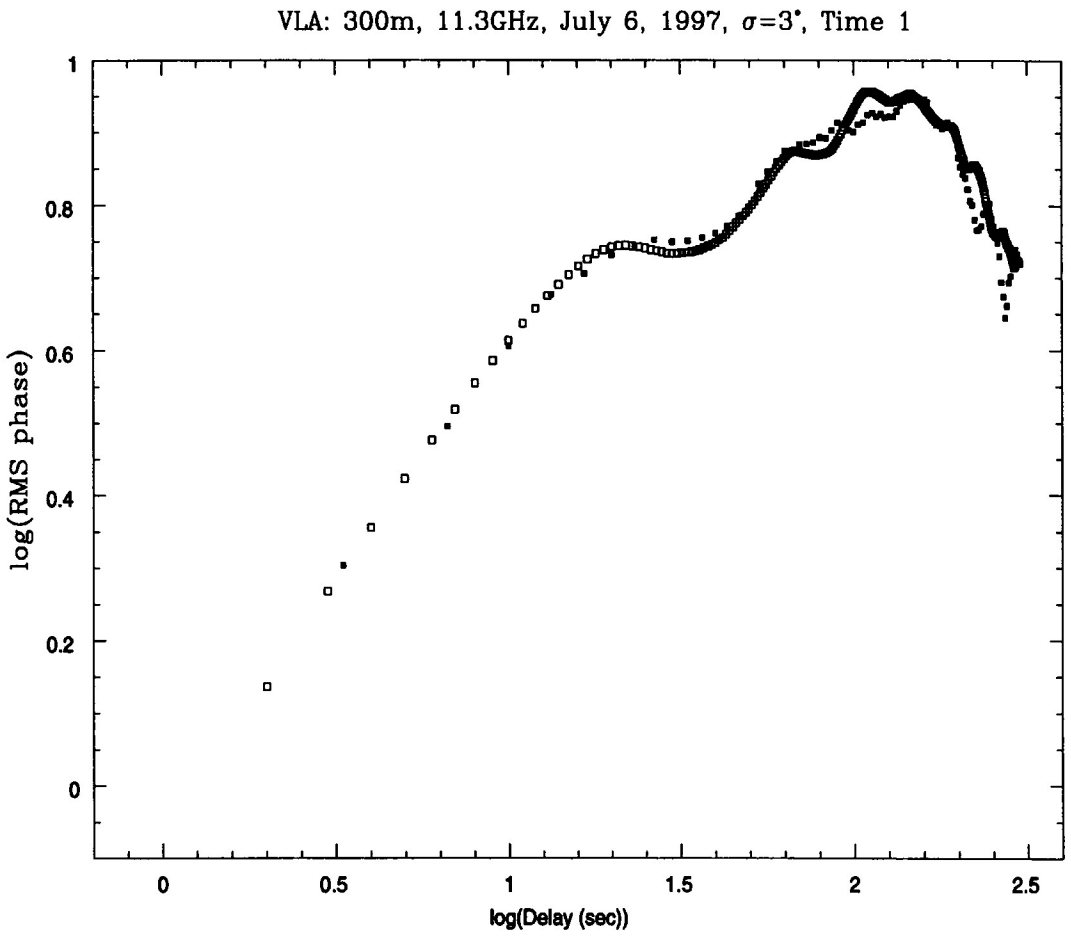

Fig. 2.— The open circles are the temporal root phase structure function from the STIfR for the 10 minutes of data around conjunction of the satellite and 2229-085 for observations on July 14, 1997. The solid squares show the temporal root phase structure function for the phases observed on the VLA baseline E4 to E8 for the same time period. Again, the VLA values have been scaled by the ratio of frequencies.

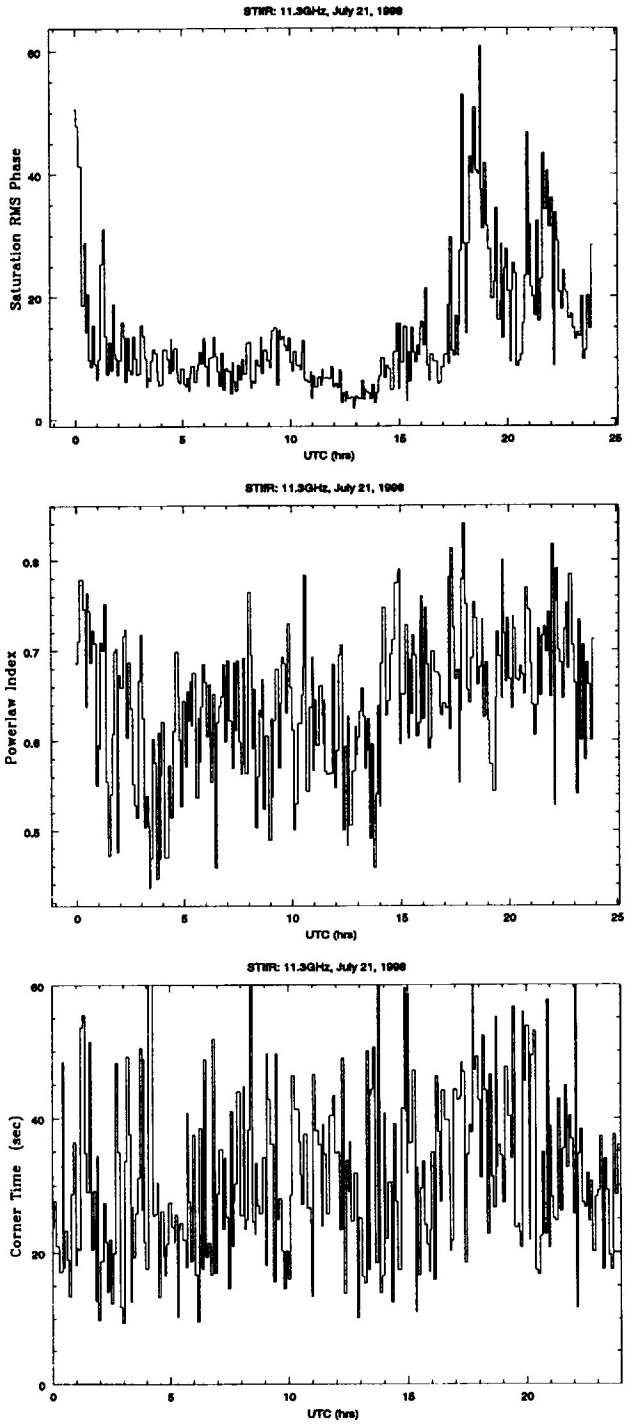

Fig. 3.— The upper plot shows the time series of the saturation rms phase of the root structure function measured by the STIfR for June 21, 1998. Entries are given every 10 min. The middle plot shows the powerlaw index, and the lower plot shows the corner time. Conjunction between the satellite and 2355-106 occured at 14:00 UTC.

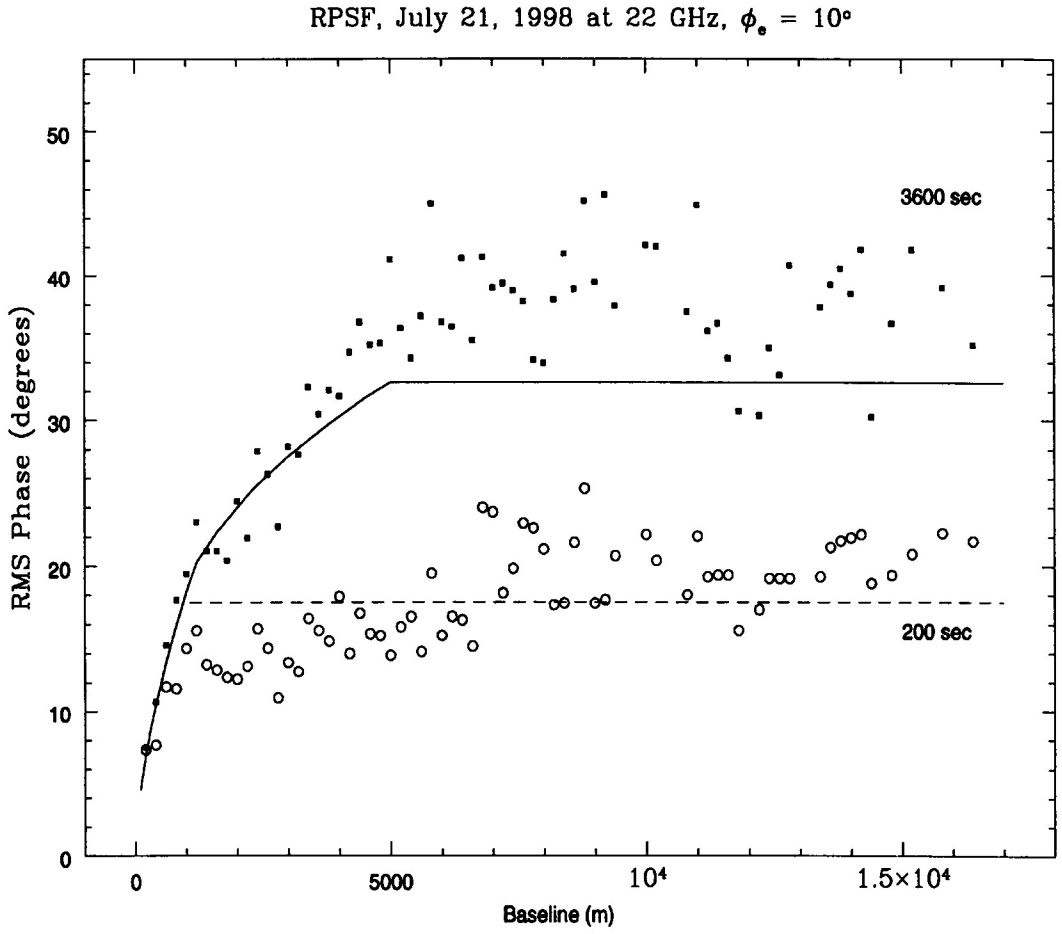

Fig. 4.— The solid squares are the spatial root phase structure function from the STIfR for the 60 min of data around conjunction for observations of the calibrator 2355-106 at 22 GHz using the BnA array of the VLA. The open circles show the root phase structure function after self-calibration with an averaging time of 200 sec. The solid line is the predicted spatial root phase structure function derived from the mean data products from the STIfR average over the observed hour around conjunction, with some assumptions about the behavior on longer baselines (W, α, and L_o). The dash line is the predicted residual root phase structure function for a calibration cycle time of 200 sec.